Japanese Journal of Applied Physics
Vol. 47, No. 7, 2008, pp. 6128–6133

Geometric Characterization of Carbon Nanotubes by Atomic Force Microscopy in Conjunction with a Tip Characterizer

Chunmei WANG[1,2], Hiroshi ITOH[1*], Yoshikazu HOMMA[3], Jielin SUN[2], Jun HU[2,4], and Shingo ICHIMURA[1]

[1]*Research Institute of Instrumentation Frontier, National Institute of Advanced Industrial Science and Technology, 1-1 Umezono 1-chome, Tsukuba, Ibaraki 305-8568, Japan*
[2]*School of Life Science and Biotechnology, Shanghai Jiaotong University, Shanghai 200240, China*
[3]*Tokyo University of Science, 1-3 Kagurazaka, Shinjuku-ku, Tokyo 162-8601, Japan*
[4]*Shanghai Institute of Applied Physics, Chinese Academy of Sciences, P.O. Box 800-204, Shanghai 201800, China*

(Received January 21, 2008; accepted April 23, 2008; published online July 18, 2008)

An atomic force microscopy (AFM) probe tip characterizer with 14 line and space structures and two knife edges was fabricated by means of a superlattice technique. The shape of a probe tip both before and after AFM imaging was acquired by this tip characterizer with general variations <1.5 nm; depending on imaging conditions. The geometric structures of carbon nanotubes (CNTs) on a SiO_2 substrate were studied by dynamic mode AFM in conjunction with this tip characterizer. Contact points between the tip and the CNTs were detected by observing changes in the AFM phase images. A modified CNT width correction model was established to calculate the estimated and upper-limit widths of two CNTs. The experimental results showed that imaging under a weak attractive force was suitable for obtaining accurate CNT height measurements, whereas a weak repulsive force provided the most accurate widths. Differing heights and widths between the two CNTs suggested that one CNT was double-walled, whereas the other had more than two walls; these results agree with transmission electron microscopy (TEM) measurements of the CNTs. [DOI: 10.1143/JJAP.47.6128]

KEYWORDS: tip characterizer, AFM, CNT, contact point

1. Introduction

Atomic force microscopy (AFM) is an important technique in nanoscience and nanotechnology because of its attractive features, including its versatility for imaging under various conditions (vacuum/air/liquid), simple sample preparation, multicharacteristic (chemical/physical) measurement capabilities, manipulation and atomic resolution capability. AFM is often used for characterizing carbon nanotubes (CNTs), which are studied extensively because of their unique mechanical and electrical properties.[1)] Unfortunately, tip-induced artifacts are a limiting factor that reduces the precision of AFM measurements and convolutes AFM data.[2)] Thorough knowledge of the shape and size of the AFM probe tip used in experiments can be helpful both for interpreting image artifacts and for enhancing the resolution. Therefore, accurate tip characterization is necessary for analysis of AFM data. Methods that are currently employed to obtain probe morphology information include scanning electron microscopy (SEM), transmission electron microscopy (TEM), blind reconstruction, and tip characterizer. However, some studies have demonstrated that the apparent morphology of CNTs as determined by dynamic mode AFM may be convoluted when the AFM tip information used in data analysis deduced from TEM results.[3)] Furthermore, potentially complex tip–sample interactions are neglected, and the high aspect ratio of CNTs also prevents a general understanding of their convolution effects in dynamic mode AFM.

In this report, we describe the fabrication of a new tip characterizer that permits both probe shape analysis and investigation of tip-induced convolution effects. This tip characterizer was fabricated by means of a superlattice technique that we developed previously,[4)] which enables the fabrication of structures with feature sizes smaller than 10 nm to be used for precisely characterizing probe tip. Our earlier studies have shown that tip characterizers created by means of the superlattice technique provide accurate probe shape information that is comparable with SEM tip characterization results. The shape of probes characterized by our new tip characterizer varied by less than 5 nm; depending on the fabrication process and imaging conditions, variations lower than 1.5 nm can be attained. The tip characterizer consisted of 14 lines and spaces ranging from 5 to 100 nm in feature size along with two knife edges, allowing the tip characterizer to be used for size correction of particles in AFM images.

We also studied CNT convolution effects by analyzing CNTs, prepared on SiO_2 substrates, by means of dynamic mode AFM with a tip characterized by our tip characterizer. The shape of the probe tip used for these AFM measurements was acquired from the new tip characterizer by taking tip–sample interactions into account.[5)] Additionally, jump-to-contact points at a single CNT were judged from phase changes observed with the characterized probe tip. The results showed that in most cases, different imaging conditions are necessary for obtaining accurate height and width for precise structural measurements of nanomaterials.

2. Experimental Procedure

A commercial AFM made by SII NanoTechnology Inc. equipped with an environmental controlling unit was used in the present experiments. All experiments were conducted in dynamic mode in air. The relative humidity (RH) was maintained at ~21%, and the temperature was maintained near 25 °C. Water layer on the surface was considered to be typically 0.2 nm.[6)] A single probe tip made of Si with a radius <7 nm and spring constant of ~1.2–3.5 N/m was used for all experiments.

Figure 1(a) is a schematic of the tip characterizer, showing lattice feature dimensions as measured from TEM images. Figure 1(b) is the corresponding SEM image. As

*E-mail address: h.itoh@aist.go.jp

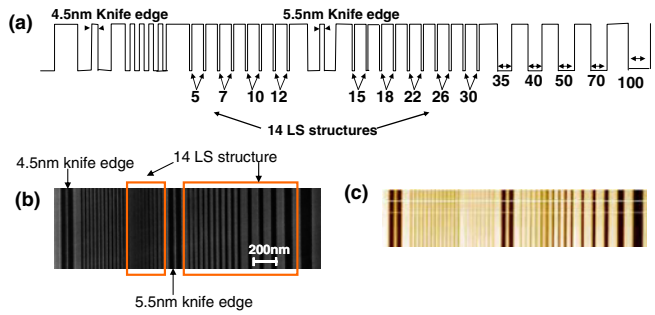

Fig. 1. (Color online) The AFM probe tip characterizer. (a) Schematic of the characterizer showing lattice feature sizes as measured by TEM; (b) SEM image of the tip characterizer; (c) AFM image of the tip characterizer, acquired with a conventional probe tip.

shown in the figure, 14 line and space (LS) structures for contrast (corrugation) transfer function (CTF) were fabricated, with widths ranging from 5 to 100 nm as measured from TEM. CTF shows the relation between probe tip width and height from probe tip apex to the bottom. Additionally, two knife edges with widths of $(4.5 \pm 0.5\,\mathrm{nm})$ and $(5.5 \pm 0.5\,\mathrm{nm})$ were fabricated. Probe shapes were acquired mainly by means of the 5.5-nm knife edge. Figure 1(c) is an AFM image of the tip characterizer, which was acquired with the tip used for characterizing CNT widths in these experiments.

To fabricate CNTs, an ultra-thin Fe film (0.4 Å) catalyst was deposited on a SiO_2 substrate by vacuum deposition. CNTs were synthesized on the substrate surface by chemical vapor deposition at 850 °C from ethanol after atmospheric heating at 400 °C for 10 min. Double-walled CNTs (DWCNTs) of ~5 nm diameter and triple-walled CNTs of ~6 nm diameter were formed, as indicated by TEM measurements.

Imaging area, where CNT is not detached from the substrate, was carefully selected. The CNTs were characterized by AFM, and the tip used to acquire the images was analyzed with the tip characterizer both before and after imaging the CNTs under proper imaging conditions.[5] To evaluate the contact point when the tip laterally approached the CNTs, reducing ratios were kept at around 20%. The free oscillation amplitude of the tip during contact point experiments was increased from 15 to 60 nm and, then, gradually decreased to 15 nm.

3. Results and Discussion

3.1 Probe shape analysis

Figure 2(a) is a typical SEM image of the probe tip used in all the experiments reported here. The SEM image was tilted by 12° which is the tilted angle of the cantilever against specimen stage. Figure 2(b) is the measured probe shape obtained from the tip characterizer knife-edge structure both before and after imaging the CNTs, as described previously.[5] The dotted points in Fig. 2(c) are the measured height–width relations from the LS structures obtained before (blue) and after (red) CNT imaging, and the inset of Fig. 2(c) shows a schematic of the LS structure measurements used to obtain the height–width relations (the plotted relations do not include the knife edge width). As shown in the figure, the relations indicated that the probe shape was

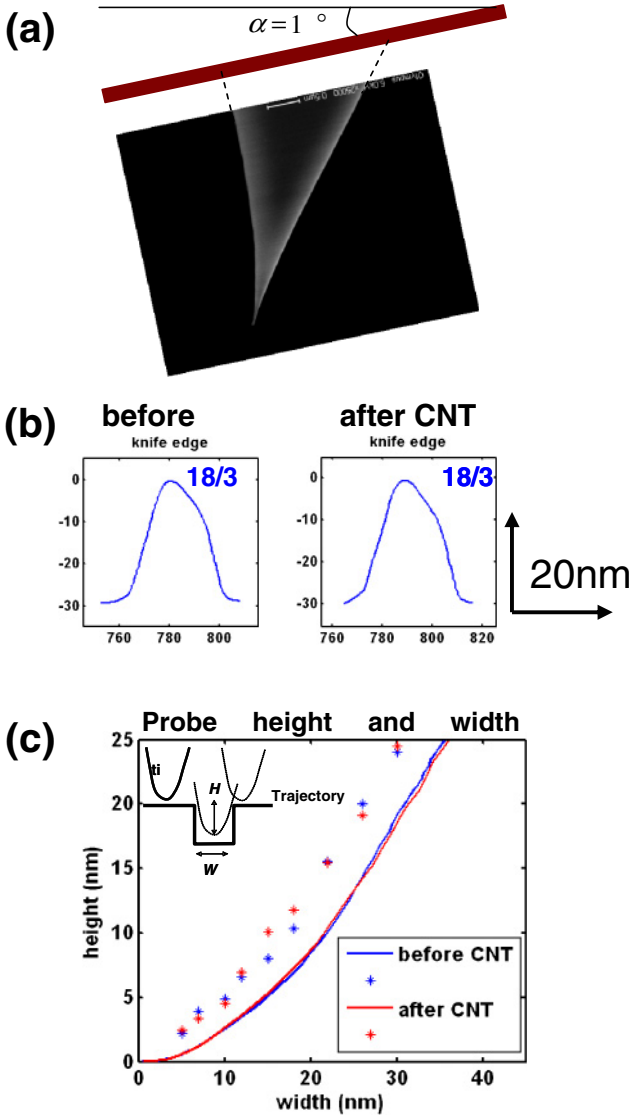

Fig. 2. (Color online) Probe shape analysis. (a) Typical SEM image of the tip used in all the experiments reported in this study. The SEM image was tilted by 12° to compensate for the tilted angle between the cantilever and the tip holder; (b) probe shape as measured from the tip characterizer knife edge structure before and after imaging CNTs; (c) height–width relations as measured from the LS structures before (blue) and after (red) the CNT imaging experiment. The inset shows a schematic of the height–width relation measurement.

almost the same before and after CNT imaging. The solid lines in Fig. 2(c) are the height–width relations determined from the knife-edge probe shape without subtracting knife-edge width, which followed the same tendency as the dotted points. It is easy to judge the degradation from height-width relations. The tip radius is lower than 5 nm, and the result shows no apparent change in the probe shape was evident after the CNTs were imaged.

Figures 3(a) and 3(b) are the probe tip shapes before and after the CNT imaging experiment. The slight differences in the slope of the probe shape between Figs. 3(a) and 3(b) might have been caused by a varying sample angle or by offline image-processing discrepancies. Considering the asymmetry of the tip, four parameters (α, β, R_1, R_2) were extracted to describe the tip, and the values of these parameters are listed in Fig. 3(c). R_1, R_2 are the curvatures of the tip apex and α, β are angles of the side wall of the probe

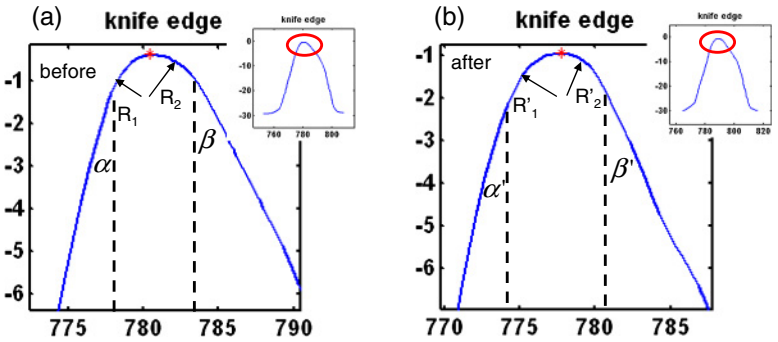

(c)

	tan α	tan β	R_1(nm)	R_2(nm)	W (nm)	H (nm)	$H'=W/(\tan\alpha+\tan\beta)$
Before	0.61	1.48	4	7.5	5	2.2	2.4
After	0.57	1.32	5.8	5.5	5	2.4	2.65

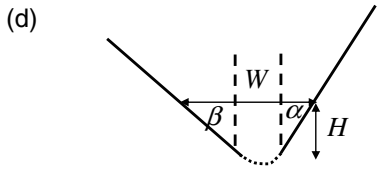

Fig. 3. (Color online) Extracted parameters from the top of the probe tip and a constructed tip model. (a) Tip shape before the CNT imaging experiment; (b) tip shape after the CNT imaging experiment; (c) table listing the four parameters (α, β, R_1, R_2) extracted from (a) and (b) to describe the tip, as well as W, H' and H; (d) model of the extracted tip shape without knife edge convolution effects.

tip. The extracted probe shapes from the knife edge structure were the result of convolution between the tip and knife edge. To obtain the true probe shape, the knife edge size should be deconvoluted. In our experiments, the knife edge was quite perpendicular, and deformation was negligible. For such a knife edge, the deconvoluted probe shape should have the same parameters α and β but smaller radii R_{1r} ($R_{1r} = R_1 - R_{\text{knife}}$) and R_{2r} ($R_{2r} = R_2 - R_{\text{knife}}$), since the knife edge radius (R_{knife}) is subtracted from R_1 for each of these radii. By setting the boundary condition for knife edge radius at the top of the tip such that both R_{1r} and R_{2r} are 0, the height (H') at a width of 5 nm was evaluated [Fig. 3(c)]. Difference between H', which is determined by knife-edge method, and H, which is determined by using 5 nm space structure, was less than 0.3 nm in this experiment. Figure 3(d) shows a model of the extracted probe shape after knife-edge width was subtracted. In this model, H and W are determined from the 5-nm LS structure and side wall of the probe tip was determined from the line profile of AFM image at the knife edge.

3.2 *Characterizing CNTs*

Figure 4(a) shows AFM images of CNTs obtained with varying values of A_{sp}/A_0, where A_{sp} is the imaging oscillation amplitude and A_0 is the free oscillation amplitude. The values of A_{sp} and A_0 used to acquire the AFM images are listed in Fig. 4(a). The reverse-phase images indicate that the CNTs were imaged in two different force regimes, that is, the attractive and repulsive force regimes, resulting in different lateral resolution,[3] as shown in topography images. Two CNTs, marked A and B in Fig. 4(a), were studied. Figure 4(b) shows the line profiles of these two CNTs under different imaging conditions.

3.3 *CNT height*

Under low free amplitude ($A_{\text{sp}}/A_0 = 6\,\text{nm}/10\,\text{nm}$), the heights of CNTs A and B were measured as 5.3 and 5 nm, respectively; at a higher free amplitude ($A_{\text{sp}}/A_0 = 18\,\text{nm}/35\,\text{nm}$), the measured height of CNT A decreased to 4.1 nm, whereas that of CNT B remained nearly the same (4.9 nm). CNT B was considered to be harder than CNT A, because it does not deform at higher force set-point. Thus, CNT B contained more graphene layers than CNT A,[7] leading to the observed discrepancies between the relative changes in the measured CNT heights with varying free amplitude. The CNT heights measured under low free amplitude were assumed to be correct. These results are similar to the results observed in other experiments reporting the AFM analysis of Au particles;[3,8] these studies also indicate that, in general, the most accurate feature height for soft materials is acquired under low free amplitude (i.e., in the attractive force regime), because the deformation of the materials is negligible.

3.4 *CNT width*

In addition to evaluating the true height of CNTs A and B from dynamic mode AFM, we tried to measure an accurate CNT width. As observed in Fig. 4(a), both CNTs A and B were imaged with better resolution at a higher free amplitude (i.e., in the repulsive force regime). Chen *et al.* have shown that acquiring images in the repulsive force regime is necessary for quantitative imaging and analysis, since imaging reaches the geometric limits in the repulsive force region.[3] However, Shapiro *et al.* have shown that localized radial deformation between the tip and the sample occurs at the point of contact and that for soft materials (tips or

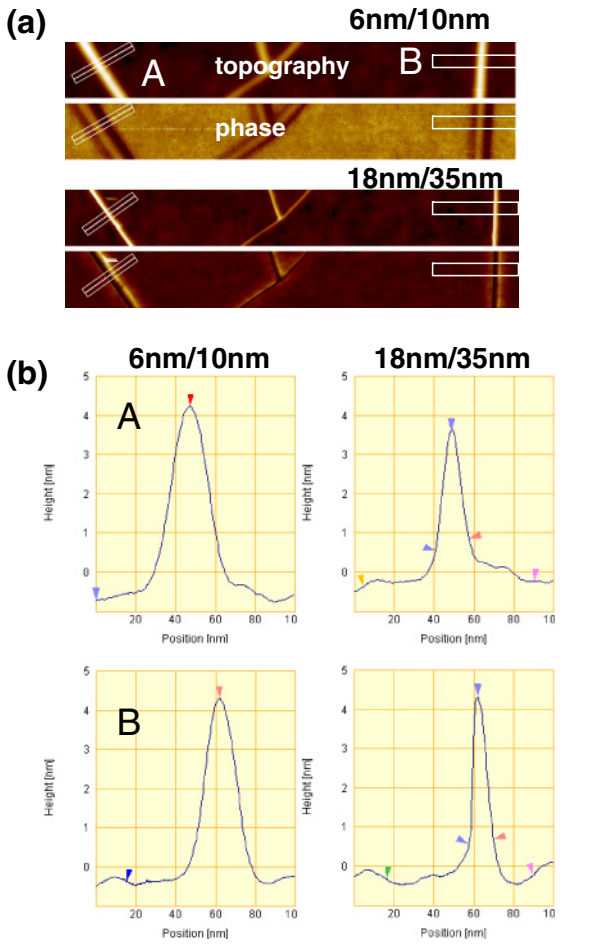

Fig. 4. (Color online) AFM images (topography and phase) of CNTs and their corresponding line profiles. (a) AFM images of CNTs acquired with different oscillation ratios (A_{sp}/A_0), denoted above the images; (b) line profiles of the two CNTs marked in (a).

samples) this radial deformation results in better convolution resolution.[9] The CNTs imaged in the present experiments experienced the same radial deformation problem when we attempted to measure their widths. Therefore, we used a contact point and sphere model to minimize the radial deformation effects in estimating the CNT widths.

3.5 *Lateral contact point judgment*

The theoretical model of convolution for AFM depicts the ideal positions when the tip touches a particle; that is, the tip is in constant contact with the sample, but repulsive forces have not yet appeared. However, some experiments have shown that when the tip scans over a particle, to maintain the cantilever oscillation amplitude at its setpoint value, either the tip or the particle will slip past the other because of bending along the length of the probe or sample and because of localized radial deformation at the contact point between the tip and the sample.[9] As the tip continues to image the sample, the tip or the sample, or both, deform to an even greater extent, which results in better convolution resolution than that predicted by theory.[10] Therefore, to achieve consistency between the theoretical model and experimental data in dynamic mode AFM, either the model or the experimental data must be adjusted to fit the other's contact conditions.[2]

Nevertheless, both experimental and theoretical studies have shown that for tip dynamics in the z-direction, the tip's interaction with the sample will progress from the non-contact to the contact state.[11] The contact point in the z-direction can be detected by a sharp phase change in the z-direction from the amplitude–distance curve.[12,13] As the tip approaches the sample from the lateral direction, the same process is observed: following contact between the tip and the sample, the repulsive force begins to increase.[9] Therefore, two contact points exist experimentally that correspond to the ideal point in the convolution model. For particles that can be modeled simply, such as spherical or fiber-like particles, a corrected or upper-limit feature size can be calculated from the contact point position if these two experimental contact points can be determined from the AFM image.

Figure 5 shows the results of an experiment designed for lateral contact point judgment. Figure 5(a) is the line profile of the topography image of the CNT B acquired with three different sets of oscillations, as described above. These sets of oscillations corresponded to the attractive force region [Fig. 5(a), top], a bi-stable state (middle) and the repulsive force region (bottom), as clearly shown by the obtained CNT images. Figure 5(b) shows the corresponding phase images of Fig. 5(a). Phase profile as shown in Fig. 5(b), the phase change due to lateral contact between the tip and the CNT is clearly observed in the middle phase profile at Fig. 5(b). As the free oscillation amplitude continued to increase, the phase change due to lateral contact became even more prominent as shown in Fig. 5(b) at the bottom profile of the phase.

We demonstrated that the phase change due to the lateral contact as shown in Fig. 5(b). The region between the dashed lines marked by the letters A and B in the linescans in Fig. 5(b) was the region in which lateral forces from the CNT affected the motion of the tip, as evidenced by the similar z-axis scale in all three linescans. Although the same regions did not show distinct transitions from non-contact to contact in the lateral direction of the topography linescans, changes in the phase in the lateral direction were more apparent. Under low free amplitude ($A_{sp}/A_0 = 12\,\text{nm}/15\,\text{nm}$), that is, in the attractive force region, the phase changed its direction twice (decreasing then increasing). In this case, the tip did not contact either the substrate or the CNT [Fig. 5(c), top]. When the tip approached the CNT in the lateral direction, the tip was lifted, and attractive forces from the substrate decreased while those from the CNT became stronger, causing the phase to decrease to a balance point before increasing as the force transitioned from substrate dominated to CNT dominated [Fig. 5(b), top]. When the free amplitude was increased to the bi-stable state [Fig. 5(b), middle], the phase initially followed the trend observed for the attractive force regime experiment but then drastically decreased, as indicated by point C in the figure. In this case, the tip initially was not in contact with the substrate or the CNT, but then a jump-to-contact was observed at some position on the CNT due to the bi-stable state [Fig. 5(c), middle], causing the phase to decrease dramatically because of the onset of repulsive forces.

As the free amplitude was increased further, the phase reversed completely [Fig. 5(b), bottom] relative to the attractive force region image (top). This phase reversal

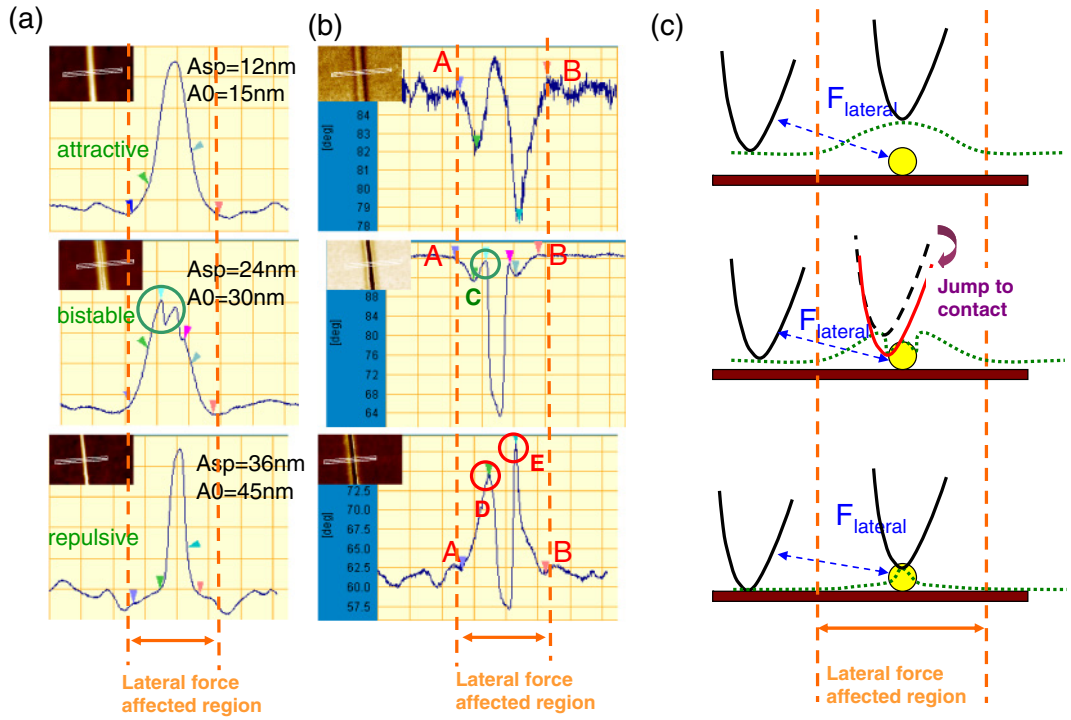

Fig. 5. (Color online) Contact point judgment as determined from dynamic mode AFM of a single CNT. (a) Line profiles of the topography image of the CNT acquired with three sets of oscillations (listed in the figure); (b) corresponding phase images and linescans; (c) schematic drawings of tip movement as deduced from the results of the three imaging conditions used in (a) and (b).

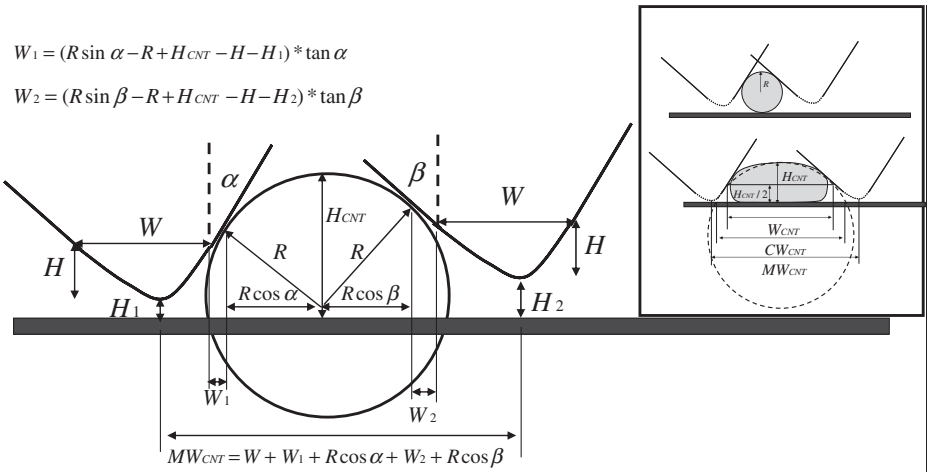

Fig. 6. Schematic drawing of the spherical CNT size-correction model.

corresponded to the state in which the tip contacted both the substrate and the CNT [Fig. 5(c), bottom]. Lateral attractive forces caused the tip to be lifted from the substrate when approaching the CNT, and the contact force in the vertical direction became weaker, corresponding to the observed increase in the phase. Contact with the CNT then resulted in a sudden decrease in phase; i.e., the transition point at which the phase direction changed corresponded to the point at which the tip initially contacted the CNT [points D and E in Fig. 5(b), bottom]. Following contact with the CNT, deformation is started.

On the basis of these results, a corrected CNT width should be calculated by imaging the CNT entirely in the repulsive force regime (i.e., with the tip in contact with both the substrate and the CNT), and the contact points should be judged from the resulting phase changes observed as the tip scans over the CNT.

3.6 *Size-correction model*

Many studies have shown that CNTs have different observed structures on substrates because the differences in the inside layers of the CNTs induce deformation on the substrate.[7,14] We used a spherical size-correction model (Fig. 6) to obtain limiting widths for these different types of CNTs (Fig. 6, inset). The real CNT width should be smaller than the maximum width of the sphere above the substrate (i.e., the corrected CNT width, CW_{CNT}, in Fig. 6) and close to the half-height width of the CNT (W_{CNT} in Fig. 6). Also shown in the size-correction model in Fig. 6 is R, the radius of the CNT, meaning that $2R$ is the corrected width of the

Table I. Parameters for CNT size correction.

	MW_{CNT} (nm)	H_1 (nm)	H_2 (nm)	H_{CNT} (nm)	R (nm)	CW_{CNT} (nm)	W_{CNT} (nm)
CNT A(b)	15.5	0.96	1.16	5.3	7.1	<13.7	~11.1
CNT A(a)	15.5	0.96	1.16	5.3	7.2	<13.8	~11.1
CNT B(b)	11.7	0.95	0.95	5	3.0	<6.0	~5.9
CNT B(a)	11.7	0.95	0.95	5	3.3	<6.6	~6.5

CNT. To calculate R, the height of the CNT (H_{CNT}), the lifted heights of the tip when contact is initiated and ceases (H_1 and H_2, respectively), the measured CNT width at the contact point (MW_{CNT}) and tip-related parameters H, W, α, and β should be extracted.

3.7 *CNT width correction*

The parameters for CNT size correction (H_{CNT}, W_{CNT}, H_1, and H_2) were extracted for both CNT A and CNT B from the AFM image under the repulsive force regime [18 nm/35 nm, Fig. 4(a)]. These parameters are listed in Table I, and the corresponding tip parameters are listed in the discussion of Fig. 3(c) above. CNT A(b) and CNT A(a) are the results determined by using probe shape before and after the CNT measurement. CNT B(b) and CNT B(a) are the resuls determined by using probe shape before and after the CNT measurement. The effective sphere radii (R) were calculated from the model shown in Fig. 6 for the probe shapes acquired before and after the CNT imaging experiments. The maximum widths of the spheres above the substrate were calculated as the upper limit of the corrected CNT width, or CW_{CNT}. W_{CNT} was the estimated width which is close to the actual CNT width.

For CNT A, the corrected width was less than 13.8 nm and close to 11 nm; for CNT B, the corrected width was less than 6.6 nm and close to 6 nm. These results indicate that CNT B was spherical and CNT A was ellipse-like shape. Therefore, CNT A was a DW-CNT and CNT B was a MW-CNT. These results also agree with the former results obtained for CNTs with similar height, which indicate that soft CNTs appear wider when affixed to a substrate because of surface van der Waals forces.[7)]

4. Conclusions

We fabricated a tip characterizer by means of a superlattice technique for characterizing the shape of an AFM probe. Geometric structures of CNTs on a SiO_2 substrate were studied by dynamic mode AFM in conjunction with this tip characterizer. The probe tip characterizer was used both before and after CNT imaging experiments to maintain the tip geometry. Changes in the AFM phase images of the CNTs were used to detect the contact point between the tip and the CNTs. A modified CNT width correction model was established to calculate estimated and upper-limit widths. Imaging in a weak attractive force region (low free amplitude) provided the most accurate height measurements, but imaging in a weak repulsive force region (high free amplitude) provided the most accurate width measurements. On the basis of the AFM images obtained for two CNTs under these different force regimes, we determined that a CNT with >2 walls was harder and more spherical (height 5 nm, width ~6 nm, maximum width <6.6 nm) than a double-walled CNT (height 5.3 nm, width ~11 nm, maximum width <13.8 nm), as expected for CNTs with varying inner-wall structures.

The method, using phase change to determine the lateral contact, can be applied to determine the actual size of the nano-materials, when tip radius is smaller than nano-materials.

Acknowledgement

This work was partially supported by the Japan Science and Technology Agency (JST).

1) I. Palaci, S. Fedrigo, H. Brune, C. Klinke, M. Chen, and E. Riedo: Phys. Rev. Lett. **94** (2005) 175502.
2) J. S. Villarrubia: J. Res. Natl. Inst. Stand. Technol. **102** (1997) 425.
3) L. W. Chen, C. L. Cheung, P. D. Ashby, and C. M. Lieber: Nano Lett. **4** (2004) 1725.
4) H. Itoh, T. Fujimoto, and S. Ichimura: Rev. Sci. Instrum. **77** (2006) 103704.
5) C. M. Wang: to be published in Dr. Thesis, School of Life Science and Biotechnology, Shanghai Jiaotong University, Shanghai.
6) D. Beaglehole and H. K. Christenson: J. Phys. Chem. **96** (1992) 3395.
7) T. Hertel, R. E. Walkup, and P. Avouris: Phys. Rev. B **58** (1998) 13870.
8) L. W. Chen, X. C. Yu, and D. Wang: Ultramicroscopy **107** (2007) 275.
9) I. R. Shapiro, S. D. Solares, M. J. Esplandiu, L. A. Wade, W. A. Goddard, and C. P. Collier: J. Phys. Chem. B **108** (2004) 13613.
10) L. A. Wade, I. R. Shapiro, Z. Y. Ma, S. R. Quake, and C. P. Collier: Nano Lett. **4** (2004) 725.
11) R. Garcia and R. Perez: Surf. Sci. Rep. **47** (2002) 197.
12) R. Garcia and A. San Paulo: Phys. Rev. B **60** (1999) 4961.
13) M. C. Strus, A. Raman, C. S. Han, and C. V. Nguyen: Nanotechnology **16** (2005) 2482.
14) R. S. Ruoff, J. Tersoff, D. C. Lorents, S. Subramoney, and B. Chan: Nature **364** (1993) 514.